CRREL
REPORT 84-3

US Army Corps of Engineers
Cold Regions Research & Engineering Laboratory

Model tests on two models of WTGB 140-foot icebreaker

USCGC KATMAI BAY

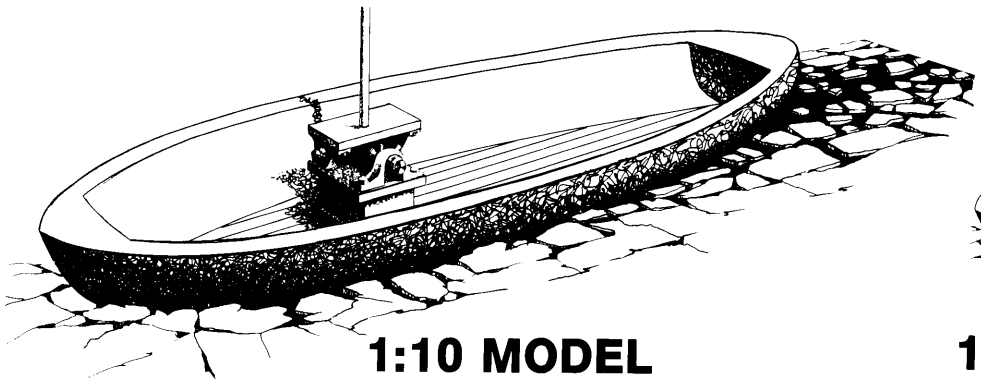

1:10 MODEL

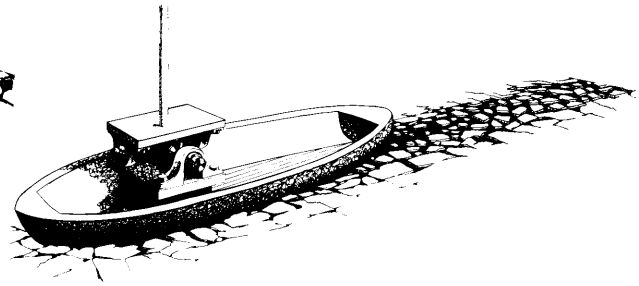

1:24 MODEL

CRREL Report 84-3

January 1984

Model tests on two models of WTGB 140-foot icebreaker

Jean-Claude Tatinclaux

Prepared for
U.S. COAST GUARD

Unclassified

SECURITY CLASSIFICATION OF THIS PAGE *(When Data Entered)*

REPORT DOCUMENTATION PAGE

READ INSTRUCTIONS BEFORE COMPLETING FORM

1. REPORT NUMBER: CRREL Report 84-3
2. GOVT ACCESSION NO.:
3. RECIPIENT'S CATALOG NUMBER:

4. TITLE *(and Subtitle)*: MODEL TESTS ON TWO MODELS OF WTGB 140-FOOT ICEBREAKER

5. TYPE OF REPORT & PERIOD COVERED:

6. PERFORMING ORG. REPORT NUMBER:

7. AUTHOR(s): Jean-Claude Tatinclaux

8. CONTRACT OR GRANT NUMBER(s): USCG Contract No. MIPR Z70099-2-06490.

9. PERFORMING ORGANIZATION NAME AND ADDRESS: U.S. Army Cold Regions Research and Engineering Laboratory, Hanover, New Hampshire 03755

10. PROGRAM ELEMENT, PROJECT, TASK AREA & WORK UNIT NUMBERS:

11. CONTROLLING OFFICE NAME AND ADDRESS: U.S. Coast Guard, 2100 2nd Street, S.W., Washington, DC 20593

12. REPORT DATE: January 1984

13. NUMBER OF PAGES: 25

14. MONITORING AGENCY NAME & ADDRESS *(if different from Controlling Office)*:

15. SECURITY CLASS. *(of this report)*: Unclassified

15a. DECLASSIFICATION/DOWNGRADING SCHEDULE:

16. DISTRIBUTION STATEMENT *(of this Report)*

Approved for public release; distribution unlimited.

17. DISTRIBUTION STATEMENT *(of the abstract entered in Block 20, if different from Report)*

18. SUPPLEMENTARY NOTES

19. KEY WORDS *(Continue on reverse side if necessary and identify by block number)*

Brash ice
Icebreaker
Ice resistance
Level ice
Model tests

20. ABSTRACT *(Continue on reverse side if necessary and identify by block number)*

The results of resistance tests in level ice and broken ice channels are presented for two models of the WTGB 140-ft icebreaker at scales of 1:10 and 1:24, respectively. No scale effect on the resistance in level ice could be detected between the two models. From the test results an empirical predictor equation for the full scale ice resistance is derived. Predicted resistance is compared against, and found to be 25 to 40% larger than, available full-scale values estimated from thrust measurements during full-scale trials of the Great Lakes icebreaker *Katmai Bay*.

DD FORM 1 JAN 73 1473 EDITION OF 1 NOV 65 IS OBSOLETE

Unclassified

SECURITY CLASSIFICATION OF THIS PAGE *(When Data Entered)*

PREFACE

This report was prepared by Dr. Jean-Claude Tatinclaux, Research Hydraulic Engineer of the Ice Engineering Research Branch, Experimental Engineering Division, U.S. Army Cold Regions Research and Engineering Laboratory. Funding for the project was provided by the U.S. Coast Guard under Contract No. MIPR Z70099-2-06490.

Dr. Malcolm Mellor and Dr. Devinder S. Sodhi, both of CRREL, were technical reviewers of the report. The author expresses his appreciation for the help and support received during the experiments from A.E. Lozeau and S.L. DenHartog. The support of the personnel of CRREL's Technical Services Division is appreciated.

CONTENTS

ILLUSTRATIONS

Figure

Tables Page

NOMENCLATURE

B	Maximum ship beam at the waterline
b	Width of cantilever beam
C_n	Dimensionless bending strength; Cauchy number = $\sigma/\gamma h_i$
E	Ice effective modulus of elasticity
f	Friction factor
$\bar{f}$	Average friction factor
F_n	Dimensionless velocity; Froude number = $V/\sqrt{gh_i}$
g	Acceleration of gravity
h_i	Ice thickness
L	Length of cantilever beam
ℓ	Ice characteristic length
N	Normal load on ice sample during friction tests
P	Normal pressure on ice sample
P_f	Failure load of cantilever beam
r	Radius of loading zone in modulus measurement; also correlation coefficient in regression analysis
R_{bk}	Breaking component of resistance in level ice
R_i	Ice resistance ($R_{it}-R_{ow}$)
R_{is}	Submergence component of resistance in level ice
R_{it}	Total resistance in ice
R_{ow}	Resistance in ice-free water
T	Tangential load on ice sample during friction tests (average friction force); also, thrust measurement
t	Thrust deduction factor
V	Ship speed
α	Ratio r/ℓ
γ	Specific weight of water
$\Delta\delta$	Displacement of ice sheet under load ΔP
ΔP	Load increment on ice sheet during modulus test
ν	Poisson's ratio of ice (= $^1/_3$)
σ	Ice flexural strength

MODEL TESTS ON TWO MODELS OF WTGB 140-FOOT ICEBREAKER

Jean-Claude Tatinclaux

INTRODUCTION

The United States Coast Guard initiated a model experimental program in ice at the U.S. Army Cold Regions Research and Engineering Laboratory (CRREL) on two models of the 140-foot WTGB at scales of 1:9.273 and 1:24, respectively. The 140-foot WTGB is a Great Lakes icebreaker designed to operate in the continuous mode of ice breaking at a speed of 3 kn (1.5 m/s) in 18 in. (46 cm) of level ice.

The larger of the two models had been tested in ice-free water at the David Taylor Naval Ship Research and Development Center (West 1975), and resistance (EHP) tests in level ice were previously conducted on the smaller model in saline model ice by ARCTEC, Inc. (Lecourt 1975). In recent years, model ice grown from an aqueous solution of urea has been adopted by a majority of ice model basins because the ratio of effective modulus E to bending strength σ that can be achieved is closer to that measured for sea ice (Timco 1980, Hirayama 1983) than that of saline model ice.

The purpose of the test program at CRREL was twofold:

1. Repeat in urea ice the EHP tests performed in saline ice by ARCTEC, Inc.

2. Assess scale effects, if any, by conducting similar tests at two different scales.

The EHP test program is to be followed by self-propulsion (SHP) tests in ice with the larger model (herein called the 1:10 model). These are for comparison with available full-scale trials data obtained with the USCGC *Katmai Bay* (Vance 1980a, Vance et al. 1981).

MODEL CHARACTERISTICS AND TEST CONDITIONS

The main characteristics of the WTGB at full scale and at the two model scales investigated are listed in Table 1. Line drawings are shown in Figure 1.

The test conditions, listed in Table 2, were limited to an ice thickness h_i of 18 in. (46 cm) full scale, an ice bending strength σ of 800-1000 kPa full scale, and to a range of velocity V of 1-5 kn (0.5-2.5 m/s) full scale.

Ice-hull coefficient of friction

The most uncertain variable in ship testing in ice may be the coefficient of dynamic friction f between the ice and the ship's hull. The basic principle in determining f consists of measuring the tangential force T against the ship's hull (or a flat plate with the same finish as the hull). The friction coefficient is taken as

$$f = T/N.$$

The exact procedures and instrumentation for applying the normal load N, pulling the ice sample along the ship's hull, and measuring T will vary from one method to another and may affect the resulting values of f. In addition, f will vary from location to location over the hull because of the difference in hull roughness due to variation in wear. Finally, different values of f will be obtained depending on whether the top or the bottom of the ice is tested, and whether there is a snow cover or not. Good examples of the effect of all these various factors on the measured values of f can be found in the report by Vance (1980) on the full-scale trial of the USCGC *Katmai Bay*.

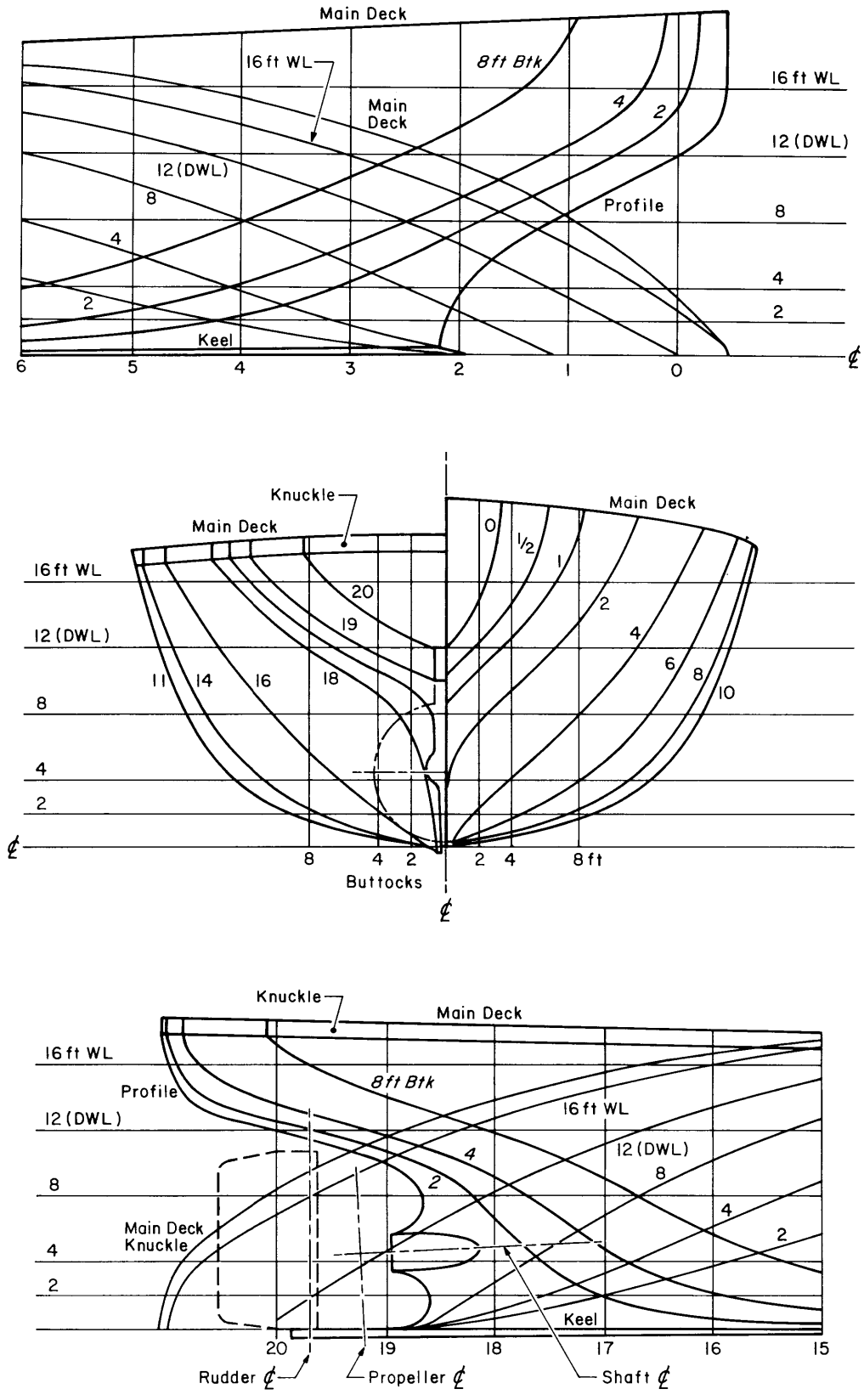

Figure 1. Abbreviated lines and body plan of USCG 140-foot WTGB.

Table 1. Principal characteristics of the *Katmai Bay* class WTGB.

Characteristic	*Description*
Length overall	140 ft (42.7 m)
Maximum beam	37 ft 6 in. (11.4 m)
Maximum beam at DWL	34 ft 2 in. (10.4 m)
Mean draft	12 ft (3.7 m)
Maximum displacement (winter)	660 metric tons (650 long tons)
Shaft horsepower	1864 kW (2500 SHP)
Maximum speed (ice-free water)	14.7 kn (7.6 m/s)
Propulsion	Twin Fairbanks Morse 38D8-1/8 diesel driving Westinghouse 1000-kW, 900-V d.c. generators, which in turn power a single Westinghouse d.c. motor coupled directly to the single propeller shaft
Auxiliaries	Two 175-kW Kato generators driven by Murphy MP24T diesels (6-cylinder, 252-hp)
Bow slope	28°
Entrance half angle at DWL	28.5°
Transverse spread angle complement	41.4°
Flare angle	48.6°

Table 2. Model test conditions.

Parameter	*1:10 model*	*1:24 model*
h_i (cm)	4.8–6.2 (45–58)	2–2.2 (47–53)
σ (kPa)	34–108 (315–1000)	33–60 (800–1400)
V (m/s)	0.23–0.84 (0.80–2.56)	0.11–0.54 (0.52–2.64)
f, ice top	0.127	0.134
f, ice bottom	0.138	0.162

Note: Numbers in parentheses are full-scale values.

As mentioned earlier, the 1:24 WTGB model had been previously tested in saline ice by ARCTEC, Inc. ARCTEC tested two models that were identical except for hull roughness. The coefficient of roughness was reported at 0.037 for the smoother model and at 0.28 for the rougher model. The exact procedure for measuring f was not given in the ARCTEC report by Lecourt (1975). In particular, the size of the ice sample is not known. However, the normal forces N applied on the ice samples (0.4–3.3 N or 0.09–0.7 lb) were quite low.

The procedure followed in the present series of tests at CRREL was as follows. A square ice sample, 7.5x7.5 in. (19x19 cm) for the 1:10 model and $3^1/_8$ x $3^1/_8$ in. (8x8 cm) for the 1:24 model, was cut from the ice sheet. The sample was inserted in a holder and set on the hull bottom, near the keel where the hull was nearly flat. The sample holder was connected via a load cell to the same motor-driven screw jack as used by Vance in the field trials of the USCGC *Katmai Bay*. The sample holder was loaded with weights, the screw jack was activated, and the pulling force on the load cell was recorded. The apparatus is sketched in Figure 2 and shown in the photographs of Figure 3. Figure 4 presents examples of friction test records. Both the top and bottom of the ice were tested, with little difference in the resulting values of f (listed in Table 3). The results also show that the friction factors for the two models were nearly equal. The overall average friction factor was

$$\bar{f} = 0.140 \pm 0.015.$$

This value is within the range 0.037–0.28 reported by ARCTEC as well as within the range 0.02 (for Inerta 160-coated steel plate) to 0.165 (for snow-covered ice against bare steel plate) reported by Vance.

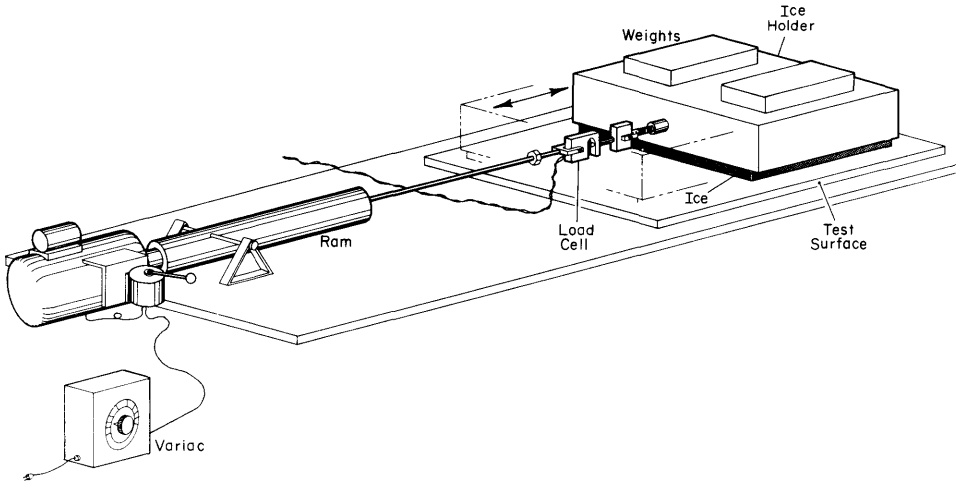

Figure 2. Diagram of friction test apparatus.

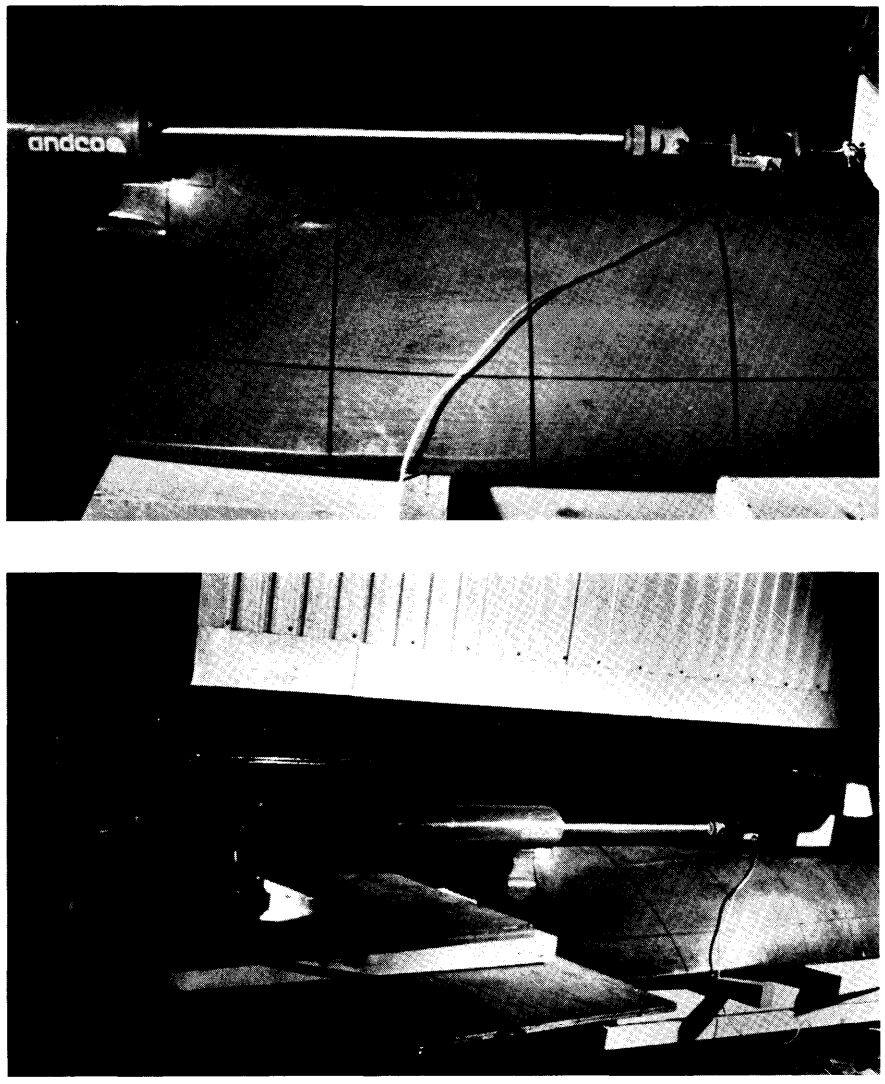

Figure 3. Friction test apparatus in operation.

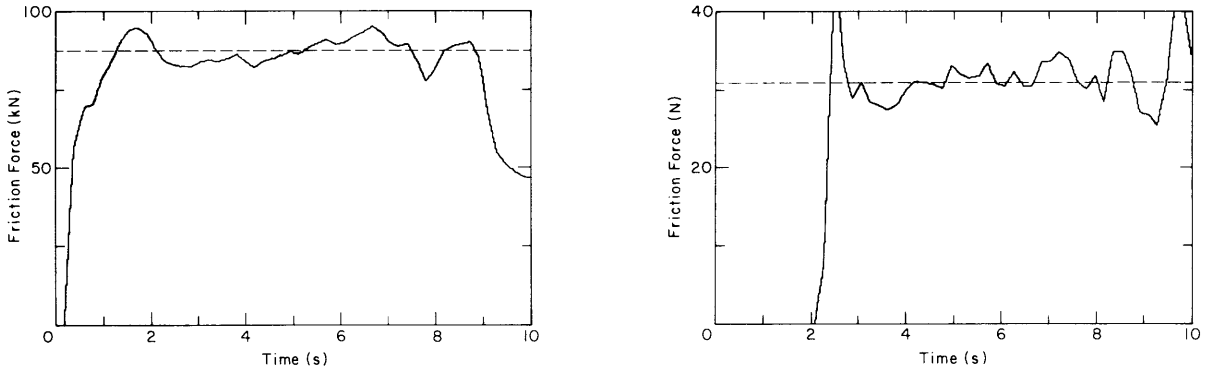

a. 1:10 model; normal load, 632 N. *b. 1:24 model; normal load, 194 N.*

Figure 4. Examples of friction test records.

Table 3. Results of friction coefficient tests.

Model	Ice surface tested	N (N)	P (kPa)	T (N)	$f = T/N$	$\bar{f}$
1:10	Bottom	632	17.5	94.7	0.150	0.138±0.0013
		632	17.5	79.2	0.125	
		632	17.5	87.2	0.138	
	Top	632	17.5	79.2	0.125	0.127±0.002
		632	17.5	80.5	0.127	
		632	17.5	80.5	0.127	
1:24	Bottom	194	30.2	31.2	0.161	0.162±0.004
		194	30.2	32.3	0.167	
		194	30.2	30.8	0.159	
	Top	194	30.2	25.1	0.130	0.140±0.015
		194	30.2	27.1	0.140	
		194	30.2	25.8	0.133	

N = normal load applied on ice sample.
P = normal pressure applied on ice sample
T = average friction force.

Measurements of ice properties

The ice thickness h_i was measured with a precision caliper with a resolution of 0.1 mm. The thickness measurements are considered to be accurate to within 0.5 mm. Before the EHP tests, the ice thickness was measured at six points along the tank periphery at about 1 m from the walls, as shown in Figure 5.

An earlier study had shown that the average of these six values gave a very good estimate of the ice thickness in the center zone of the tank (Hirayama 1983). After the tests in level ice, the ice thickness was measured at 5-m (16.25-ft) intervals along the ship track (see Fig. 5) to check ice thickness uniformity and to obtain accurate data, since it is known that ship resis-

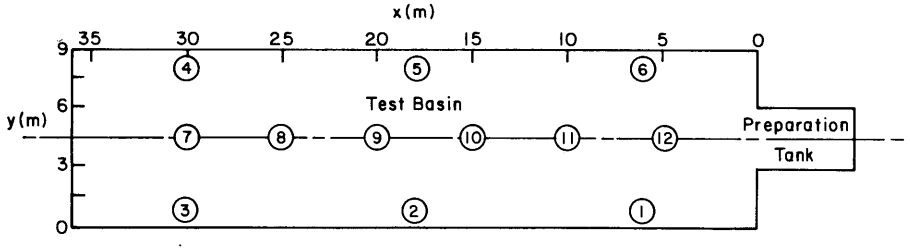

Figure 5. Basin locations of ice thickness and strength measurements. Circled numbers indicate locations where ice properties were measured.

tance in ice is very sensitive to variations in thickness.

The ice flexural strength σ was measured in situ from small cantilever beam tests. The beam length L was 5 to 7 times its thickness, and the beam width b was 1 to 2 times its thickness. The load was applied manually with a hand-held gauge with a capacity of 1 kg (2.2 lb), in such a manner that beam failure occurred within 1 or 2 seconds from initial load application. With this procedure the formula for a simple cantilever beam is valid, namely

$$\sigma = \frac{6P_f L}{b h_i^2} \tag{1}$$

where P_f is the failure load. Prior to the EHP tests in level ice, the ice strength was measured at three locations (1, 2, and 3 in Fig. 5) along the basin south wall. In most cases, ice strength measurements were also conducted after the tests along the ship track. At each location, two to three beams were usually tested.

The effective modulus of elasticity of the ice E was determined by the method described in Sodhi et al. (1982). A load is applied in incremental steps ΔP over a circular area of radius r near the center of the ice sheet. The resulting incremental deflection $\Delta\delta$ of the ice sheet at the center of the load area is measured by an LVDT (linear variable differential transformer). The characteristic length ℓ of the ice is then calculated as

$$\ell = \left\{\frac{\Delta P}{8\gamma\Delta\delta}\left[1+\frac{\alpha^2}{2\pi}\left(\ln\frac{\gamma\alpha}{2}-\frac{5}{4}\right)\right]\right\}^{1/2} \tag{2}$$

from which the effective modulus is obtained by

$$E = \frac{12(1-\nu^2)\gamma\ell}{h_i^3}. \tag{3}$$

In eqs 2 and 3, γ is the specific weight of water, ν is the Poisson's ratio of the ice taken equal to $^1/_3$, $\alpha = r/\ell$, and $\ln\gamma = 0.5577$ is the Euler's constant. The ice modulus E was determined immediately prior to the tests in level ice.

The average values of σ, h_i, and E applicable to each test are given in Tables 6 and 7 together with the test results discussed below.

EXPERIMENTAL PROCEDURES

During the tests, the ship models were free to roll, pitch, and heave. They were limited in sway and totally restrained in surge. In both models the pitch axis was located slightly forward of the ship's center of gravity; the pitch axis could not pass through the center of gravity because of space requirements for the installation of the variable-speed motor and the thrust and torque dynamometer to be used in subsequent SHP tests with the 1:10 model. For the 1:10 model, the center of rotation in roll was some 6 in. (15 cm) above the center of rotation in pitch. The towing mechanism for the 1:24 model, specially built for the present tests, was designed such that the centers of rotation in pitch and roll coincided. These towing mechanisms are shown in Figure 6.

Data acquisition system

In the EHP tests with both models, only the resistance force was measured. A 250-lb (1100-N) capacity force block was used for the 1:10 model with a resolution of ±0.5 lb (±2 N). A 50-lb (220-N) capacity force block was used for the 1:24 model with a resolution of ±0.1 lb (±0.5 N). Both force blocks are models H1-M-4, manufactured by Hydronautics, Inc. The voltage signal from the force block was digitized by a NEFF-602 multiplexer and signal conditioner at sampling intervals of 5 to 15 ms, depending upon the towing speed. It was recorded in digital form on floppy disks for later analysis. The analog signal was also recorded on magnetic tape, as a backup, and on a Gould Model 260 strip chart recorder. Typical force records are shown in Figure 7. The overall data acquisition system is outlined in Figure 8.

Test program and procedures for 1:10 model

The 1:10 model was 15 ft long (4.6 m). To ensure at least two ship lengths of testing at constant towing speed, and to allow sufficient distance for acceleration and deceleration of the carriage, only two towing speeds could be tested per ice sheet. A total of 14 tests (seven ice sheets) were made; two tests were conducted at each of the three nominal full-scale speeds of 1.5, 4, and 5 kn (0.8, 2.1, and 2.6 m/s) and four tests were run at each of the two full-scale speeds of 2 and 3 kn (1.0 and 1.5 m/s). For each ice sheet, in addition to EHP tests in level ice, EHP tests in brash ice were also conducted at the same speed conditions as in level ice, as described below.

For each ice sheet the test procedure was as follows: The model was towed at the first selected speed over the first half-length of the tank; the ship was backed over one model length to leave room for acceleration for the second test run over the second half-length of the tank. Once the tests in level ice were completed, the model was returned to the trim tank. The channel left in the ice by the model was then refilled manually with broken ice floes as completely as possible, so as to form a single layer of floes. The model was then

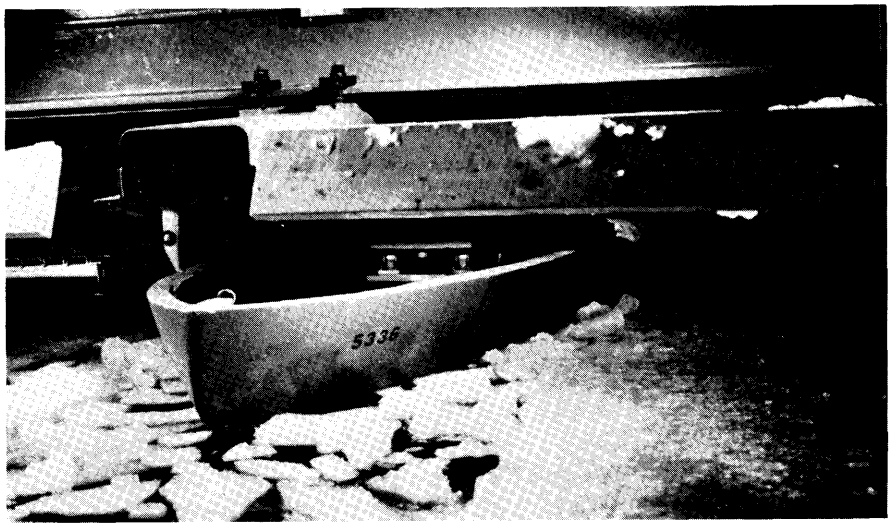

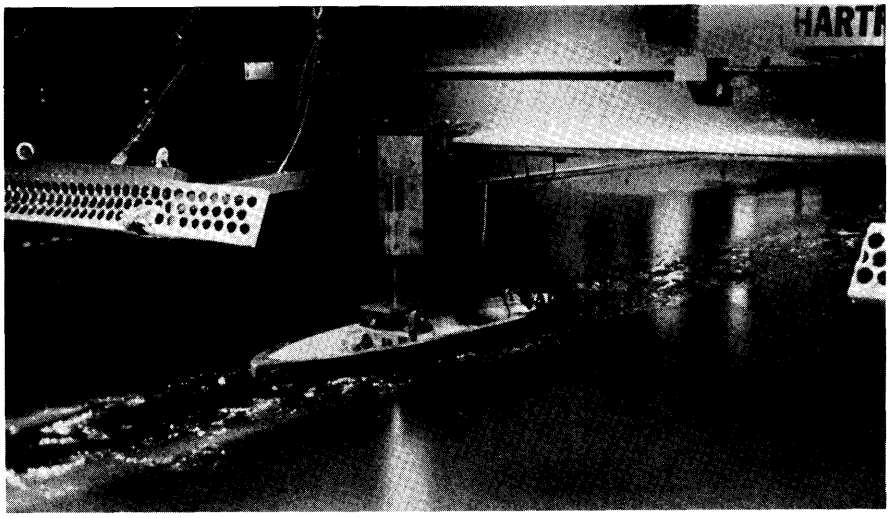

b. 1:24 model.

Figure 6. Models under testing.

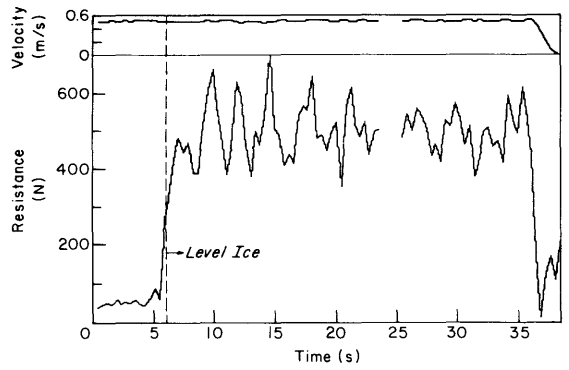

a. 1:10 model: h_i *= 6 cm,* S *= 80 kPa,* V *= 0.53 m/s.*

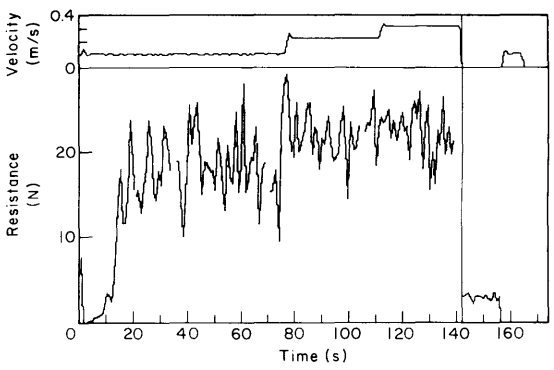

b. 1:24 model: h_i = 2 cm, *S = 30 kPa,* V *= 0.11, 0.22, 0.32 m/s.*

Figure 7. Examples of test records.

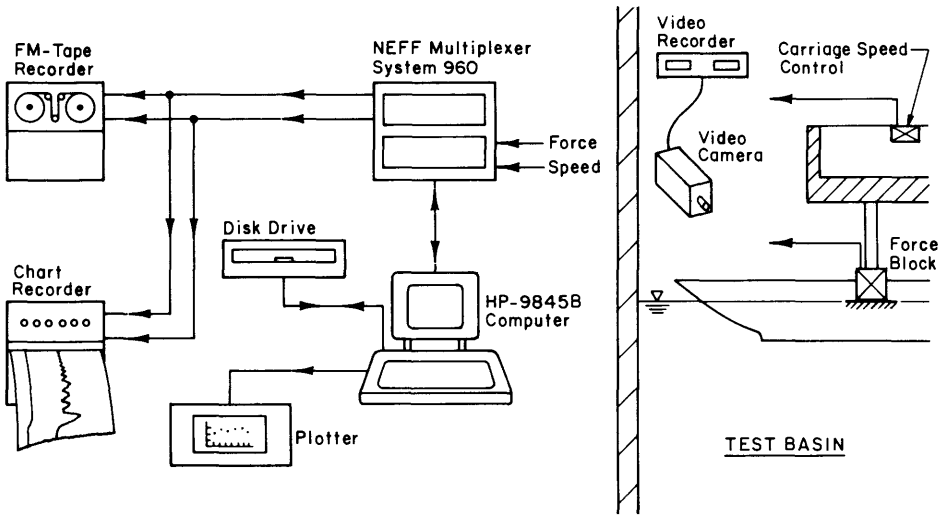

Figure 8. Diagram of the data acquisition system.

Table 4. Test program for 1:10 model.

Ice sheet	*Level ice test*	*Brash ice test*	*Nominal full-scale speed (kn)*	*Distance along test basin (m)*	*No. of ship lengths*
1	101	151	1.5	0–14	3.0
	102	152	2.0	14–28	3.0
2	103	153	2.0	0–14	3.0
	104	154	3.0	14–28	3.0
3	105	155	3.0	0–14	3.0
	106	156	4.0	14–30	3.5
4	107	157	3.0	0–16	3.5
	108	158	5.0	16–30	3.0
5	109	159	4.0	0–16	3.5
	110	160	5.0	16–30	3.0
6	111	161	3.0	0–14	3.0
	112	162	2.0	14–28	3.0
7	113	163	2.0	0–14	3.0
	114	164	1.5	14–28	3.0

towed through this brash ice at the same speeds and over the same distances as in the level ice tests. The test program for the 1:10 model is given in Table 4.

Test program and procedures for 1:24 model

Because of the small size of this model—approximately 6 ft (1.8 m) long and 18 in. (0.45 m) in beam—the five speeds to be investigated could be tested along two parallel tracks in one ice sheet. In a first series of tests the model was suspended from the carriage as close as possible to one wall of the trim tank, which is 10 ft (3 m) wide. Either the three model speeds corresponding to 1, 2, and 3 kn full scale or the two speeds corresponding to 4 and 5 kn full scale were run continuously by changing the speed setting from one value to the next with the carriage in motion (see Fig. 7b).

The 1:10 model was tested first, and it was observed that the ice floes broken by the model re-emerged in the wake, after immersion and sliding along the model, and almost reoccupied their initial position. A fair description of the track left in the ice by both models would be a completed puzzle with little water visible (see Fig. 9). Since the 1:24 model was relatively light (100 lbs or 450 N), and there was enough clearance between the bottom of the carriage and the ice surface, the model could be lifted out of

a. 1:10 model.

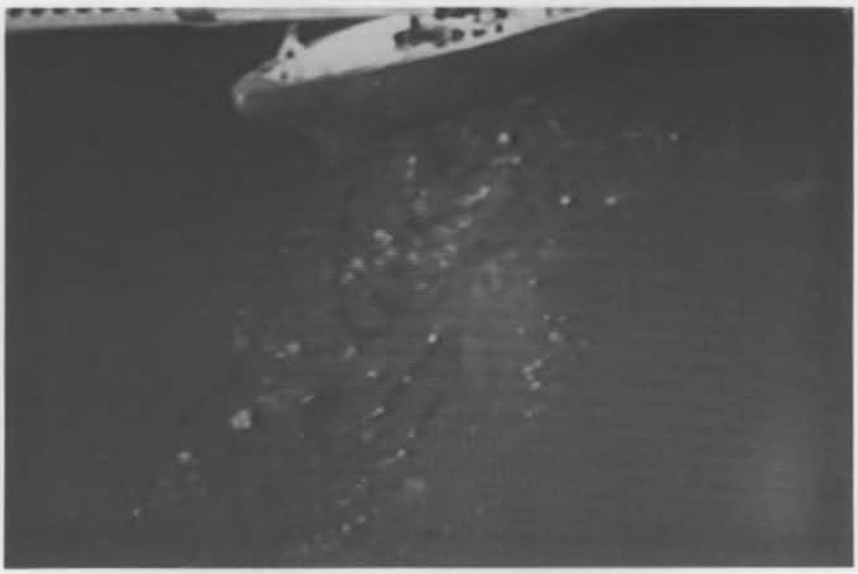

b. 1:24 model.

Figure 9. Photographs of tracks behind models in level ice.

the water and ice and carried back to the trim tank, leaving the broken channel undisturbed (see Fig. 9, bottom). The model was then towed through the undisturbed broken ice track at the same speeds as in the level ice tests.

Once the model had been run through the ice sheet at the first set of speeds, it was moved to the other side of the trim tank and tests were conducted for the remaining speeds. This procedure was impossible with the 1:10 model because of its size. Its width (44 in. or 1.12 m) precluded tests along two parallel tracks, and its weight and draft made it impossible to lift the model out of the ice and return it to the trim tank while leaving the broken channel undisturbed.

When the experimental data was analyzed, it was found that the relative resistance of the 1:24 model in

Table 5. Test program for 1:24 model.

a. Tests in level ice and undisturbed broken channels.

Ice sheet	*Level ice test*	*Broken channel test*	*Nominal full-scale speed (kn)*	*Distance along test basin (m)*	*No. of ship lengths*
1a	201	251	1	0–8	4.5
	202	252	2	8–16	4.5
	203	253	3	16–24	4.5
1b	204	254	4	2–12	6.0
	205	255	5	12–24	7.0
2a	206	256	3	0–12	7.0
	207	257	2	12–22	6.0
	208	258	1	22–30	4.5
2b	209	259	5	0–16	9.5
	210	260	4	16–30	8.5
3a	211	261	4	0–13	8.0
	212	262	5	13–30	10.0
3b	213	263	3	0–14	8.5
	214	264	2	14–24	6.0
	215	265	1	24–30	3.5

b. Additional tests in brash and pre-sawed ice (one ice sheet).

Type of test	*Test*	*Nominal full speed (kn)*	*Distance along basin (m)*	*No. of ship lengths*
Pre-sawed channels 1	301	4	0–8	4.5
	302	5	8–14	3.5
	303	3	14–22	4.5
	304	1	23–26	3.5
	305	1	26–33	4.0
Pre-sawed channels 2	306	1	0–6	3.5
	307	2	6–12	3.5
	308	3	12–18	3.5
	309	5	18–25	4.0
	310	4	25–32	4.0
Brash-filled channels 1	311	4	0–8	4.5
	312	5	8–15	4.0
	313	3	15–21	3.5
	314	2	22–28	4.0
	315	1	28–33	3.0
Brash-filled channels 2	316	1	0–5	3.0
	317	2	5–11	3.5
	318	3	11–18	4.0
	319	5	18–25	4.0
	320	4	25–32	4.0
Unconfined brash	321	1	0–5	3.0
	322	2	5–11	3.5
	323	3	11–18	4.0
	324	5	18–25	4.0
	325	4	25–32	4.0

the undisturbed broken channel was about twice that of the 1:10 model in the brash-filled channel. This discrepancy needed further investigation and the following additional sets of experiments were conducted with the 1:24 model.

a. Tests in pre-sawed ice channels. A channel slightly wider than the model beam was manually sawed in the level ice.

b. Tests in brash-filled channels. After completion of the tests in pre-sawed channels, the model was towed

back, the ship track was manually refilled with ice floes, and the tests were repeated. This procedure nearly duplicated the tests in brash-filled channels conducted with the larger model.

c. Tests in unconfined brash-filled channel. After completion of the tests in brash-filled channels, the adjacent ice was broken manually to widen the channel to about three to four times the model beam. The widened channel was filled with a single layer of floes and the tests were repeated.

The entire test program for the 1:24 model is listed in Table 5.

ANALYSIS OF TEST RESULTS

The EHP test data obtained with the 1:10 model are listed in Table 6, and for the 1:24 model in Table 7. In these tables, R_{it} is the total measured resistance in ice and R_{ow} is the resistance in ice-free water estimated from the test results given by West (1975) by

$$R_{ow} = 13.84\ V^{2.02} \quad \text{for 1:10 model} \qquad (1a)$$

$$R_{ow} = 2.6\ V^{2.05} \quad \text{for 1:24 model} \qquad (1b)$$

where V is the velocity in m/s and R_{ow} is in newtons. The level ice resistance was calculated as $R_i = R_{it} - R_{ow}$. It can be noted that the ice-free resistance R_{ow} is extremely small compared to R_{it} and could have been neglected without significantly affecting the analysis of the data.

In Tables 6 and 7, the ice resistance was normalized by $\gamma B h_i^2$ where γ is the specific weight of water taken equal to 9.81 kN/m^3, B is the ship model's maximum beam at the waterline, and h_i is the ice thickness. The dimensionless bending strength, or Cauchy number, was defined as $C_n = \sigma/\gamma h_i$ and the dimensionless velocity, or Froude number, as $Fn = V/\sqrt{g h_i}$.

Comparison of test results between 1:10 and 1:24 models

The dimensionless ice resistance in level ice obtained with both models is plotted versus the product $(C_n \cdot F_n)$ on Figure 10. It can be seen that the results obtained with one model are in remarkable agreement

Table 6. Results of EHP tests with 1:10 model.

Test	h_i (cm)	V (m/s)	σ (kPa)	E (mPa)	R_{it} (N)	R_{ow} (N)	R_i (N)	$Fn = V/\sqrt{gh_i}$	$\sigma/\gamma h_i$	$R_i/\gamma B h_i^2$
					a. In level ice					
101	5.05	0.26	38	76	186.0	0.9	185	0.36	76	6.58
102	4.98	0.32	34	76	195.7	1.4	194	0.46	70	7.11
103	6.09	0.32	80	171	394.5	1.4	393	0.41	134	9.62
104	6.22	0.50	80	171	504.3	3.4	501	0.64	131	11.75
105	5.00	0.50	78	143	286.5	3.4	283	0.71	159	10.27
106	4.99	0.66	83	143	336.5	6.0	331	0.94	169	12.04
107	4.92	0.50	88	108	269.5	3.4	266	0.72	182	9.97
108	4.85	0.84	88	108	309.8	9.7	300	1.22	185	11.58
109	4.88	0.66	98	166	362.1	6.0	356	0.95	204	13.57
110	4.90	0.84	88	166	369.2	9.7	360	1.21	183	13.59
111	5.15	0.50	96	154	356.5	3.4	353	0.70	190	12.08
112	5.47	0.35	101	154	387.0	1.7	385	0.48	188	11.68
113	5.51	0.35	94	218	452.2	1.7	451	0.48	174	13.46
114	5.51	0.26	108	218	442.3	0.9	441	0.35	200	13.19
					b. In brash-filled channel					
151	5.05	0.26			46.9	0.9	46	0.36		1.64
152	4.98	0.32			53.6	1.4	52	0.46		1.91
153	6.09	0.32			46.9	1.4	46	0.41		1.11
154	6.22	0.50			62.6	3.4	59	0.64		1.39
155	5.00	0.50			41.8	3.4	38	0.71		1.39
156	4.99	0.66			55.5	6.0	50	0.94		1.80
157	4.92	0.50			39.6	3.4	36	0.72		1.36
158	4.85	0.84			67.2	9.7	58	1.22		2.22
159	4.88	0.66			49.3	6.0	43	0.95		1.65
160	4.90	0.84			61.1	9.7	51	1.21		1.94
161	5.15	0.50			49.8	3.4	46	0.70		1.59
162	5.47	0.35			54.3	1.7	53	0.48		1.60
163	5.51	0.35			56.6	1.7	55	0.48		1.64
164	5.51	0.26			49.4	0.9	49	0.35		1.45

Table 7. Results of EHP tests with 1:24 model.

Type of test	Test	h_i (cm)	V (m/s)	σ (kPa)	E (mPa)	R_{it} (N)	R_{ow} (N)	R_i (N)	$F_n = V/\sqrt{gh_i}$	$\sigma/\gamma h_i$	$R_i/\gamma B h_i^2$
					a. In level ice						
Level ice	201	2.17	0.11	33	26	18.0	0.0	18.0	0.23	153	8.97
	202	2.15	0.23	38	26	21.8	0.1	21.7	0.50	180	11.02
	203	2.12	0.32	38	26	22.0	0.2	21.8	0.71	182	11.37
	204	2.22	0.41	38	26	26.5	0.4	26.1	0.89	173	12.44
	205	2.17	0.53	42	26	26.7	0.7	26.0	1.14	196	12.97
	206	1.96	0.31	39	31	18.7	0.2	18.5	0.72	202	11.29
	207	1.96	0.23	42	31	18.9	0.1	18.8	0.51	218	11.48
	208	1.96	0.11	45	31	15.0	0.0	15.0	0.24	236	9.16
	209	2.11	0.54	52	31	29.2	0.7	28.5	1.19	250	15.04
	210	2.10	0.41	60	31	26.9	0.4	26.5	0.91	291	14.12
	211	2.03	0.40	38	27	23.1	0.4	22.7	0.91	192	12.94
	212	2.01	0.53	38	27	21.9	0.7	21.2	1.19	192	12.33
	213	2.08	0.31	40	27	22.2	0.2	22.0	0.70	197	11.92
	214	2.06	0.23	45	27	20.9	0.1	20.8	0.50	222	11.50
	215	2.07	0.11	45	27	14.8	0.0	14.8	0.23	222	8.10
					b. In broken pre-sawed, or brash-filled channel						
Broken channel	251	2.11	0.11			5.0	0.0	5.0	0.23		2.51
	252	2.15	0.23			5.0	0.1	4.9	0.50		2.48
	253	2.12	0.32			5.1	0.2	4.9	0.71		2.56
	254	2.22	0.41			6.0	0.4	5.6	0.89		2.65
	255	2.17	0.53			7.3	0.7	6.6	1.14		3.28
	256	1.96	0.31			4.3	0.2	4.0	0.72		2.14
	257	1.96	0.23			4.4	0.1	4.3	0.51		2.77
	258	1.96	0.11			3.7	0.0	3.7	0.24		2.60
	259	2.11	0.54			7.8	0.7	7.1	1.19		3.75
	260	2.10	0.41			6.3	0.4	5.9	0.91		3.13
	261	2.03	0.40			5.3	0.4	4.9	0.91		2.80
	262	2.01	0.53			5.9	0.7	5.2	1.19		3.01
	263	2.08	0.31			5.2	0.2	5.0	0.70		2.69
	264	2.06	0.32			5.6	0.1	5.4	0.50		3.01
	265	2.07	0.11			3.3	0.0	3.3	0.23		1.81
Pre-sawed channels 1	301	2.42	0.41			5.8	0.4	5.4	0.83		2.14
	302	2.43	0.52			7.8	0.7	7.1	1.07		2.84
	303	2.43	0.31			5.8	0.2	5.7	0.64		2.25
	304	2.41	0.23			5.6	0.1	5.5	0.46		2.22
	305	2.42	0.11			4.7	0.0	4.7	0.22		1.88
Pre-sawed channels 2	306	2.82	0.11			3.8	0.0	3.8	0.22		1.12
	307	2.76	0.23			5.5	0.1	5.4	0.44		1.66
	308	2.64	0.32			5.9	0.2	5.7	0.62		1.91
	309	2.59	0.53			9.7	0.7	9.0	1.06		3.14
	310	2.58	0.41			7.3	0.4	6.9	0.82		2.43
Brash-filled channels 1	311	2.42	0.41			8.3	0.4	7.9	0.84		4.05
	312	2.43	0.52			10.9	0.7	10.2	1.07		3.16
	313	2.43	0.31			7.5	0.2	7.3	0.64		2.90
	314	2.41	0.23			6.9	0.1	6.8	0.46		2.75
	315	2.42	0.11			7.3	0.0	7.3	0.22		3.05
Brash-filled channels 2	316	2.82	0.11			5.8	0.0	5.8	0.20		1.70
	317	2.76	0.23			9.6	0.1	9.5	0.44		2.93
	318	2.64	0.32			7.7	0.2	7.4	0.62		2.50
	319	2.51	0.54			12.1	0.7	11.4	1.07		4.00
	320	2.58	0.41			9.1	0.4	8.8	0.82		3.08
Unconfined brash	321	2.76	0.11			5.2	0.0	5.2	0.20		1.61
	322	2.75	0.23			6.5	0.1	6.4	0.44		2.00
	323	2.72	0.32			6.2	0.2	6.0	0.61		1.86
	324	2.72	0.54			10.5	0.7	9.8	1.04		3.12
	325	2.73	0.41			7.1	0.4	7.5	0.08		2.35

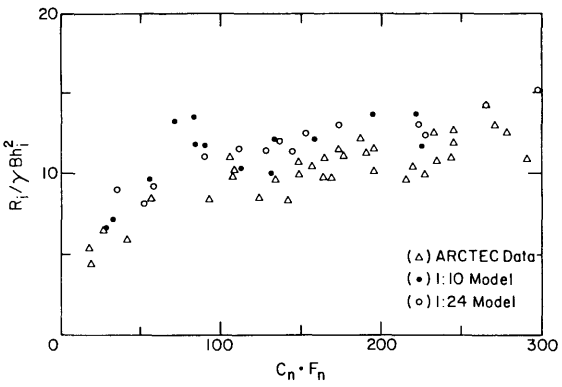

Figure 10. Comparison of resistance in level ice between the two models (dimensionless).

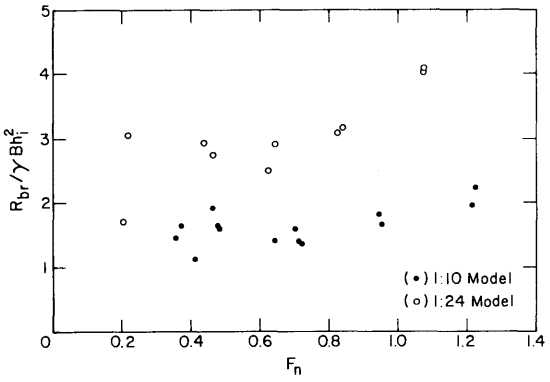

Figure 11. Comparison of resistance in brash-filled channel between the two models.

with those obtained with the other model. This indicates that, for the range of experimental parameters investigated (velocity, ice thickness, ice strength), no scale effect on the ice resistance in level ice can be detected between the two models. The results obtained in the ARCTEC tests in saline ice (Lecourt 1975) are also plotted on Figure 10; they show excellent agreement with those of the present study.

When the dimensionless resistance in brash-filled channels is plotted against the Froude number F_n as in Figure 11, it can be seen that the resistance obtained with the 1:24 model is approximately twice that measured with the 1:10 model. This large discrepancy between the two sets of data is puzzling especially in view of the previously good agreement of the results in level ice. No satisfactory explanation can be offered at this time, and only conjectures can be proposed:

a. There are indeed scale effects between the two models, both in the resistance through ice and in the breaking component of the level ice resistance, of opposite magnitude such that the net effect on the total resistance in level ice is negligible at the particular model scales studied here.

b. In performing the tests in brash-filled channels with the 1:10 model, the channels were not fully filled and significant open water areas were left.

c. In towing back the 1:10 model and manually refilling the channel, ice floes were broken into pieces that were relatively smaller than those resulting from a similar operation with the 1:24 model. The corresponding difference in aspect ratio of the ice floes would lead to a change in submergence behavior, added masses, etc. and in the overall resistance of the ship models.

d. There was a systematic error in the force measurements, which could be of the same absolute magnitude for both models, but that would be relatively larger for the 1:24 model in brash ice where the level of the measured forces is quite small.

e. A combination of b, c, and d above.

Analysis of tests in broken or brash-filled ice channels

The results of the tests performed with the 1:24 model in broken ice following the various procedures described earlier are shown in Figure 12. In spite of the scatter, the ice resistance in broken ice appears to be little affected by the particular procedure followed (undisturbed broken channel in level ice, pre-sawed channel, brash-filled, or unconfined brash). Furthermore, the results of tests through an undisturbed broken channel with the 1:24 model show excellent repeatability, as evidenced by Figure 13, where the results obtained for three different ice sheets have been plotted.

It was therefore considered that the test results of the 1:24 model in the undisturbed broken channel

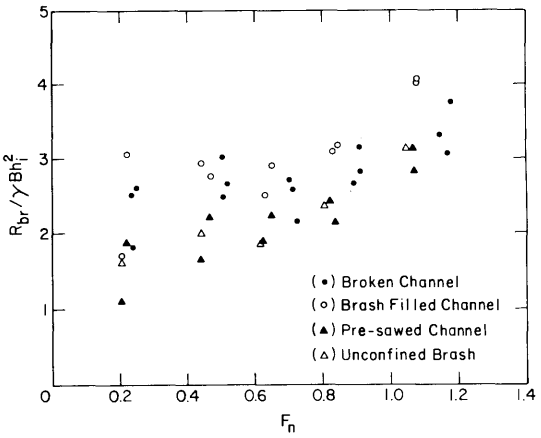

Figure 12. Resistance in broken ice for different procedures (1:24 model).

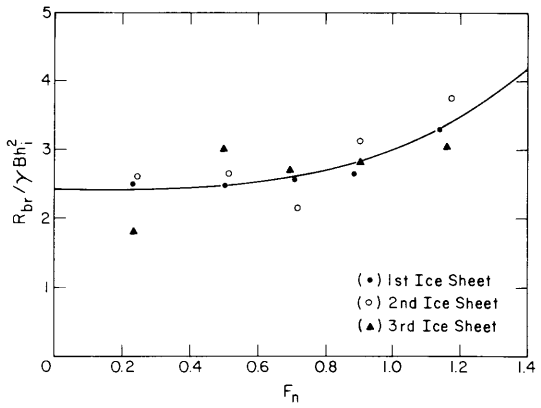

Figure 13. Resistance in undisturbed broken channel through three ice sheets (1:24 model).

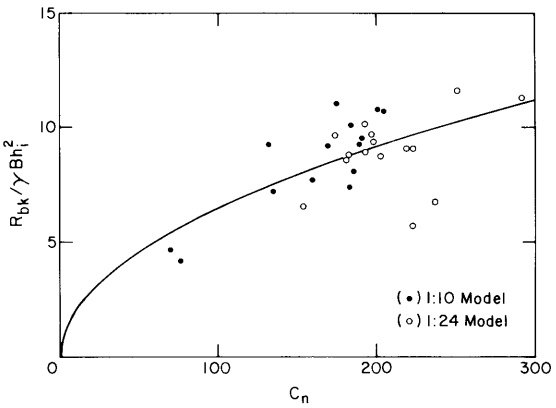

Figure 14. Dimensionless breaking resistance as a function of Cauchy number.

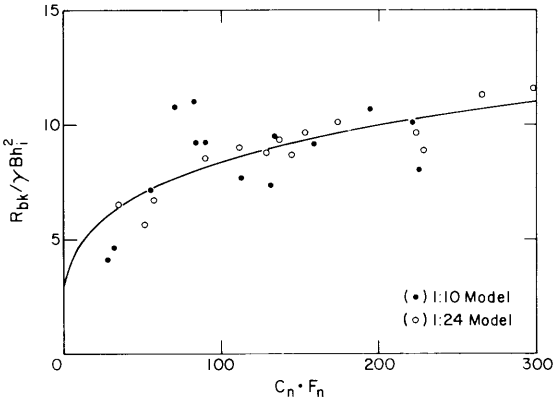

Figure 15. Dimensionless breaking resistance as a function of $C_n \cdot F_n$.

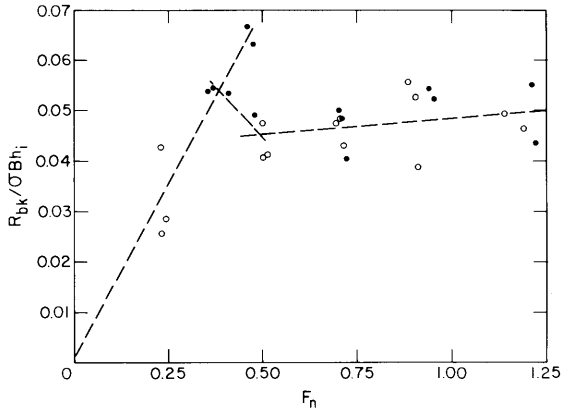

Figure 16. Plot of $R_{bk}/\sigma Bh_i$ *as a function of* F_n *(dimensionless quantities).*

were representative of the submergence and inertia components on the total ice resistance in level ice. A nonlinear regression analysis of the data presented in Figure 13 yielded the equation

$$\frac{R_{is}}{\gamma Bh_i^2} = 2.28 + 0.784\left(\frac{V}{\sqrt{gh_i}}\right)^2. \qquad (2)$$

This equation, derived from the tests with the 1:24 model, was assumed to be also valid for the 1:10 model, pending further testing of this latter model in broken channels.

Analysis of tests in level ice

The ice-breaking resistance was taken as the difference between the measured resistance in level ice R_i and the submergence resistance R_{is} given by eq 2, namely

$$\frac{R_{bk}}{\gamma Bh_i^2} = \frac{R_i}{\gamma Bh_i^2} - \frac{R_{is}}{\gamma Bh_i^2}. \qquad (3)$$

It is usually considered that the dimensionless breaking resistance is primarily a function of the Cauchy number, that is, that ice failure occurs essentially in bending. The values of the dimensionless breaking resistance obtained for both models according to eq 3 are plotted vs Cauchy number C_n on Figure 14. If a power function is fitted through the data, the following equation is obtained

$$\frac{R_{bk}}{\gamma Bh_i^2} = 0.653\left(\frac{\sigma}{\gamma h_i}\right)^{0.5} \qquad (5)$$

with a correlation coefficient $r = 0.71$.

From his test results with the 1:24 model, Lecourt (1975) concluded that the resistance data correlated best with the product $(C_n \cdot F_n)$. In following that second approach, the dimensionless breaking resistance was plotted vs $(C_n \cdot F_n)$ on Figure 15, which yielded the following relationship

$$\frac{R_{bk}}{\gamma B h_i^2} = 2.69\,(C_n \cdot F_n)^{0.25} \qquad (6)$$

with a correlation coefficient $r = 0.78$.

The third approach in the analysis of the breaking resistance was as follows. If the assumption that ice failure occurs primarily in bending is indeed correct, then the breaking resistance should be proportional to σ and h_i, and the quantity $R_{bk}/\sigma B h_i$ should be independent of C_n and a function of F_n only. This new dimensionless quantity was plotted vs the Froude number on Figure 16. From this figure it is apparent that $R_{bk}/\sigma B h_i$ initially increases rapidly with the Froude number, reaches a maximum, and drops rapidly to an almost constant value. In view of the scatter in the data points, it was considered sufficient to divide the data into three zones, for which the following linear equations were obtained

$$\frac{R_{bk}}{\sigma B h_i} = 0.01 + 0.115 F_n, \quad F_n < 0.4 \qquad (7a)$$

$$\frac{R_{bk}}{\sigma B h_i} = 0.1 - 0.11 F_n, \quad 0.4 < F_n < 0.5 \qquad (7b)$$

$$\frac{R_{bk}}{\sigma B h_i} = 0.042 + 0.0063 F_n, \quad F_n > 0.5. \qquad (7c)$$

The transition Froude number range $F_n = 0.4$–0.5 corresponds, for a full-scale ice thickness of 18 in. (46 cm), to a full-scale speed range of 1.7–2.1 kn (0.87–1.08 m/s). It might be noted that during the model tests the amplitude of the pitching motion was relatively high for speeds of 1, 1.5, and 2 kn (full-scale equivalent) and it decreased rapidly at higher speeds, so much so that, at the nominal full-scale speeds of 4 and 5 kn, the ship model took a practically constant trim angle. The loss of energy due to these pitching and heaving motions would result in additional resistance. As the ship speed increases, the additional resistance due to pitching decreases so that the total ice resistance may actually decrease over a narrow range of speed or Froude number before the monotonically increasing inertia component of the resistance overcomes this effect. Such a reversal in the ice resistance curve has been observed before (e.g. by Schwarz 1977) and predicted theoretically by Milano (1973) and is sometimes called the "Milano hump." It would be useful to perform additional tests in the range of Froude number 0.1–0.75 to confirm the observed hump and to better define the behavior of the breaking resistance with the Froude number in this range.

FULL-SCALE PREDICTION OF LEVEL ICE RESISTANCE

Combining eq 2 with either eqs 5, 6, or 7 yields three predictors for the level ice resistance, viz.

Predictor I:

$$\frac{R_{it}}{\gamma B h_i^2} = \frac{R_{ow}}{\gamma B h_i^2} + 2.28 + 0.784\left(\frac{V}{\sqrt{g h_i}}\right)^2 + 0.653\left(\frac{\sigma}{\gamma h_i}\right)^{0.5}$$

Predictor II:

$$\frac{R_{it}}{\gamma B h_i^2} = \frac{R_{ow}}{\gamma B h_i^2} + 2.28 + 0.784\left(\frac{V}{\sqrt{g h_i}}\right)^2 + 2.69\left(\frac{\sigma}{\gamma h_i} \cdot \frac{V}{\sqrt{g h_i}}\right)^{0.25}$$

Predictor III:

$$\frac{R_{it}}{\gamma B h_i^2} = \frac{R_{ow}}{\gamma B h_i^2} + 2.28 + 0.784\left(\frac{V}{\sqrt{g h_i}}\right)^2 + \frac{\sigma}{\gamma h_i}\left(a + b\frac{V}{\sqrt{g h_i}}\right)$$

with $a = 0.01$ and $b = 0.115$ for $F_n < 0.4$; $a = 0.1$ and $b = -0.1$ for $0.4 < F_n < 0.5$; and $a = 0.042$ and $b = 0.0063$ for $F_n > 0.5$.

Because the above equations are empirical relationships derived from model test results, they are valid only for the range of parameters investigated, namely

$$0.23 < F_n < 1.22$$

and

$$75 < (\sigma/\gamma h_i) < 300$$

or

$$30 < C_n \cdot F_n < 300.$$

From the results of the resistance tests conducted at NSRDC (West 1975), the full-scale ice-free resistance was estimated by

$$R_{ow} = 78.6\,V^{2.13} \qquad V < 5 \text{ m/s}$$

$$R_{ow} = 53.9\,V^{3.83} \qquad 5 \text{ m/s} < V < 7.2 \text{ m/s}$$

with R_{ow} expressed in N and V in m/s. The accuracy in R_{ow} is not critical since it is but a small part of the total resistance in level ice, especially at speeds below 5 kn (2.5 m/s) modeled in the present study.

The model data and the full-scale trial values of resistance in level ice reported by Vance (1980) are plotted in Figure 17 for comparison. In Figure 18, the dimensionless form of the resistance measured

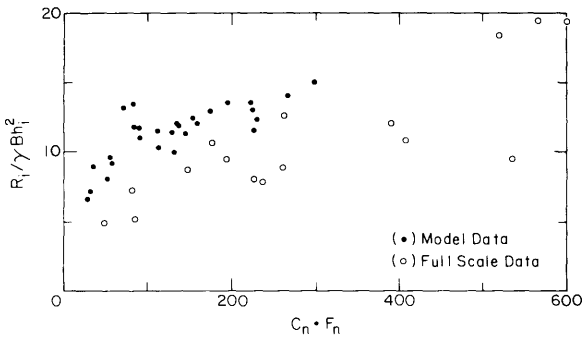

Figure 17. Comparison between model test results and full-scale data.

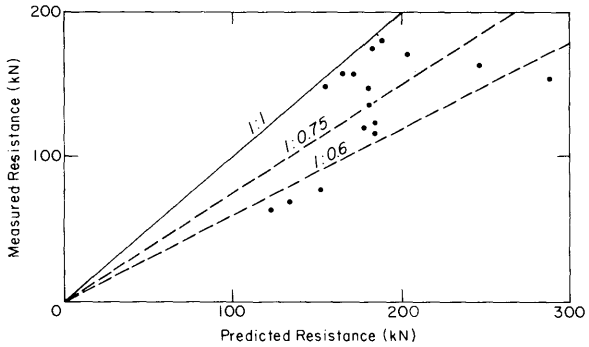

Figure 18. Comparison between full-scale resistance predicted by Predictor III and trials data.

Table 8. Summary of full-scale trials data in level ice. Extracted from Vance (1980b).

h_i (in.)	σ* (lb/ft^2)	V (kn)	R_{it}† (lb)	$\frac{R_{it}}{\gamma Bh_i^2}$	Run no.	Date
12.0	12737	1.4	15386	7.21	1000	30 Jan 79
15.0	12110	5.6	26827	8.05	1010	
11.0	12528	7.8	33278	18.56	1020	
11.0	12110	8.8	35304	19.69	1030	
14.0	13781	0.98	14135	4.87	1100	31 Jan 79
14.5	13781	5.4	27700	8.89	1110	
14.0	13572	10.59	34369	11.83	1120	
15.0	13572	8.99	36548	10.96	1130	
15.0	(12946)	5.48	26000	7.80	1200	
13.0	(12946)	7.28	30470	12.17	1210	
11.0	12946	8.78	35277	19.64	1220	
15.0	(13363)	1.94	17203	8.16	1300	9 Feb 79
16.0	(13363)	3.64	33000	8.70	1310	
16.5	(13363)	5.01	38323	9.47	1320	
16.0	(13363)	4.35	40416	10.65	1330	
14.5	13363	5.58	39194	12.58	1331	

*Values in parentheses were not measured but assumed equal to the value measured in one run of the series.
†Calculated as $(1-t)T$ where T was the measured thrust and the value of the thrust deduction factor t taken equal to 0.2.

during the trials is plotted against the resistance calculated by Predictor III for the trial conditions of ice thickness, ice strength, and ship speed (listed in Table 8). From both Figures 17 and 18 it is evident that the model results lead to significantly higher resistance than measured in the full-scale trials. However, it is worth noting that the trial data in Figure 18 can be divided into two groups, one where the measured resistance is 75% or more of the predicted value, the second where the full-scale resistance is in the order of 60% of the predicted values. These two groups of data correspond to two series of trials conducted on two different days at two different locations. In addition, the full-scale trials resistance data were estimated from thrust measurements T as

$$R = (1-t)T$$

with the thrust deduction factor t taken equal to 0.2. Therefore, comparison of the model test results with the full-scale data may be premature and should await the results of future SHP tests with the 1:10 model.

CONCLUSIONS

1. The tests performed on two models of the 140-foot WTGB icebreaker showed that, within the range of parameters investigated, the dimensionless ice resistance in level ice was essentially the same for both models. This lack of scale effect proves that, for this class of icebreaker, initial resistance tests in ice can be conducted with small models, at a scale of approximately 1:25, during early design efforts. Such early testing should prove worthwhile in optimizing hull shape for icebreaking efficiency and ice floe motion pattern in the stern area.

2. The results obtained in the present study in urea ice are in very close agreement with those from earlier tests by ARCTEC, Inc., in saline ice. This indicates that both model ices are satisfactory, at least for the model scales and range of parameters investigated.

3. Tests in level ice and broken ice allowed the ice resistance to be divided into a submergence-inertia component and an ice-breaking component. It was found that the ice-breaking component was proportional to the Cauchy number, $\sigma/\gamma h_i$, as expected, but it was also influenced by the Froude number, $V/\sqrt{gh_i}$. In particular, a rapid change in the ice-breaking resistance was found to occur at a Froude number of 0.4-0.5. For the range of $F_n < 0.4$ and $F_n = 0.4$-0.5, the

resistance increased rapidly with F_n. It decreased somewhat in the vicinity of $F_n = 0.475$, and was a weakly linearly increasing function of F_n for $F_n >$ 0.5. This behavior was tentatively attributed to the corresponding observed change in the amplitude of the pitching and heaving motions of the ship models.

4. Comparison of the test results with the few full-scale trial data available indicated that the model resistance in level ice was significantly larger than the full-scale measurements. It remains unclear whether the observed discrepancy is in fact present since, during the field trials, the ice-hull friction coefficient could not be determined with confidence, measurement of the ice strength was not performed for all tests and had to be estimated, the ice thickness could only be spot-checked, and the presence of undetected cracks in the ice would weaken it and result in lower resistance.

5. On the basis of the results of the present model tests, it would be helpful to conduct additional tests in broken ice with the larger 1:10 model, in level ice in the range $F_n = 0.3$–0.6 to confirm the observed behavior of the ice-breaking resistance. If these latter tests are performed, the pitching and heaving motions of the ship models should be measured.

LITERATURE CITED

Hirayama, K. (1983) Properties of urea-doped ice in the CRREL test basin. USA Cold Regions Research and Engineering Laboratory, CRREL Report 83-8. ADA128219.

Lecourt, E.J. (1975) Icebreaking model tests of the 140-foot WYTM. ARCTEC, Inc., Report 202 C-2.

Milano, V.R. (1973) Ship resistance to continuous motion in ice. *Transactions, Society of Naval Architects and Marine Engineers,* **81**: 274-306.

Schwarz, J. (1977) New developments in modeling ice problems. *Proceedings, POAC 77, St. John's, Newfoundland,* 45-61.

Sodhi, D.S., K. Kato, F.D. Haynes, and K. Hirayama (1982) Determining the characteristic length of model ice sheets. *Cold Regions Science and Technology,* **6**: 99-104.

Timco, G.W. (1980) The mechanical properties of saline-doped and carbamide urea-doped model ice. *Cold Regions Science and Technology,* **3**: 45-56.

Vance, G.P. (1980a) Analysis of the performance of a 140-foot Great Lakes icebreaker: USCGC *Katmai Bay.* USA Cold Regions Research and Engineering Laboratory, CRREL Report 80-8.

Vance, G.P. (1980b) Supplementary data for analysis of the performance of a 140-ft Great Lakes icebreaker (USCGC *Katmai Bay*). USA Cold Regions Research and Engineering Laboratory, Internal Report 621 (unpublished).

Vance, G.P., M.J. Goodwin, and A.S. Graiewski (1981) Full-scale icebreaking test of the USCGC *Katmai Bay. Proceedings, Sixth STAR Symposium, SNAME, Ottawa, Canada,* 323-343.

West, E.E. (1975) Powering predictions for the United States Coast Guard 140-foot WYYM presented by Model 5336. NSRDC Report SPD-233-16.